Symmetric and asymmetric ternary fission of hot nuclei

K. Siwek-Wilczynska
Kernfysisch Versneller Instituut, 9747 AA Groningen, The Netherlands
and Institute of Experimental Physics, Warsaw University, 00-681 Warsaw, Poland

J. Wilczynski
Kernfysisch Versneller Instituut, 9747 AA Groningen, The Netherlands
and Soltan Institute for Nuclear Studies, 05-400 Swierk-Otwock, Poland

H. K. W. Leegte, R. H. Siemssen, and H. W. Wilschut
Kernfysisch Versneller Instituut, 9747 AA Groningen, The Netherlands

K. Grotowski, A. Panasiewicz, Z. Sosin, and A. Wieloch
Institute of Physics, Jagellonian University, 30-059 Cracow, Poland
and Institute of Nuclear Physics, 31-342 Cracow, Poland
(Received 11 February 1993)

Emission of α particles accompanying fusion-fission processes in the $^{40}Ar + ^{232}Th$ reaction at $E(^{40}Ar) = 365$ MeV was studied in a wide range of in-fission-plane and out-of-plane angles. The exact determination of the emission angles of both fission fragments combined with the time-of-flight measurements allowed us to reconstruct the complete kinematics of each ternary event. The coincident energy spectra of α particles were analyzed by using predictions of the energy spectra of the statistical code CASCADE. The analysis clearly demonstrates emission from the composite system prior to fission, emission from fully accelerated fragments after fission, and also emission during scission. The analysis is presented for both symmetric and asymmetric fission. The results have been analyzed using a time-dependent statistical decay code and confronted with dynamical calculations based on a classical one-body dissipation model. The observed near-scission emission is consistent with evaporation from a dinuclear system just before scission and evaporation from separated fragments just after scission. The analysis suggests that the time scale of fission of the hot composite systems is long (about 7×10^{-20} s) and the motion during the descent to scission almost completely damped.

PACS number(s): 25.70.Jj

I. INTRODUCTION

The dynamics of nucleus-nucleus fusion reactions and deexcitation of hot composite systems formed in these reactions have attracted much interest in recent years. Special attention has been paid to heavy composite systems in which light-particle decay modes compete with fission over a wide range of excitation energies.

The energy distributions of light charged particles (protons, α particles) detected in coincidence with compound-residue nuclei and/or fission fragments give valuable information on the dynamics of the deexcitation cascade (see, e.g., Refs. [1,2]). The spectra of α particles taken in coincidence with fission fragments usually can be separated into a part corresponding to the emission prior to fission and that after scission, i.e., the emission from fully accelerated fragments. In a few papers [3–7], it was, however, suggested that the coincident spectra additionally contain a third component that can be interpreted as corresponding to the emission of α particles during the fission process, i.e., at a near-scission configuration. The third component therefore can be viewed as an analogue of ternary fission known from extended studies of spontaneous fission and neutron-induced fission at low excitation energies (see [8,9] and references therein).

In the present paper, we report on an exclusive experiment that imposed sufficiently strong restrictive conditions (ternary coincides, determination of the mass asymmetry of the fission fragments, many α-particle detection angles) that allowed us to unambiguously identify the events of practically simultaneous ternary division. We confirm the previous observations [3–7] of the near-scission emission (NSE) and give estimates of the probability (α multiplicities) of this component for both symmetric and asymmetric fission. Moreover, we demonstrate that the relative strength of the near-scission emission provides important information on the dynamics of fission.

II. EXPERIMENTAL TECHNIQUE

In the present experiment, ternary fission events were studied in the $^{40}Ar + ^{232}Th$ reaction. An $^{40}Ar^{(11+)}$ beam of 365 MeV from the KVI isosynchronous cyclotron bombarded a ^{232}Th target of 1.5 mg/cm^2 thickness. Fission fragments were detected in two position-sensitive avalanche detectors (PSAD's) [10] of a sensitive area of 200×140 mm^2, positioned symmetrically on both sides of the beam axis, with their centers placed at the angles $\theta_{f1}=55°$ and $\theta_{f2}=-55°$. The PSAD's were moved to a

sufficiently large distance of 35 cm from the target to allow us to determine the time of flight of the fission fragments with a satisfactory accuracy. The time of flight was measured with respect to the rf signal of the cyclotron. The phase stability of this signal with respect to the beam burst on the target was controlled by recording the time signal of elastically scattered ^{40}Ar particles in the monitor detector. In an off-line analysis, the time signals from the fission detectors were corrected for the observed changes of the monitor detector timing. The scale of the time-of-flight measurements was calibrated by assuming that the average kinetic energy of the observed fission fragments is given by the updated systematics of Viola, Kwiatkowski, and Walker [11].

Light charged particles accompanying fission events were detected in ten low-threshold telescopes [12] placed in the backward hemisphere, eight of them in the average fission plane at $\theta_\alpha = 120°$, 130°, 140°, 150°, 160°, 170°, $-170°$, and $-160°$. Two detectors were placed out of the fission plane at $\theta = -170°$ and $\phi = 40°$ and 60°. The telescopes had a gas ΔE section backed by a large-area (1200 mm^2) Si(Li) detector. The telescopes were calibrated by measuring between the coincidence runs the known α-decay lines from the ^{232}Th target material serving by itself as a very convenient calibration source. In such a way, the stability of the detectors response, pressure of gas, effective thickness of the target seen from each detection angle, etc. were perfectly under control.

III. EXPERIMENTAL RESULTS

The exact determination of the emission angles of both fission fragments combined with the time-of-flight measurements allowed us to reconstruct the complete kinematics of each ternary event involving two fission fragments and a light fragment detected in one of the backward-angle telescopes. We limit the present analysis to the most frequent events when the detected light fragment is an α particle.

The α particles detected in coincidence with fission fragments may be emitted from (i) the composite system prior to fission, (ii) during fission, i.e., from the near-scission configuration, or (iii) well after scission—from fully accelerated fragments. In the following analysis, we attempt to unambiguously identify mechanism (ii) and estimate its intensity relative to mechanism (i). Since α emission in stages (ii) and (iii) depends on the mass of the fission fragments, the analysis of the triple f-f-α events was done separately for symmetric and asymmetric fission.

For each event the measured velocity vectors v_1 and v_2 of the fission fragments were transformed to the reference frame of the fissioning nucleus. The collinearity of the transformed velocities, $v_1^{\text{c.m.}}$ and $v_2^{\text{c.m.}}$, was checked, and their relative magnitudes were used for the determination of the mass asymmetry:

$$M_1/(M_1+M_2) = v_2^{\text{c.m.}}/(v_1^{\text{c.m.}}+v_2^{\text{c.m.}}) . \quad (1)$$

The mass distribution for all the triple f-f-α events is shown in Fig. 1. Three regions in this distribution have been chosen for the analysis: $M_1/M = 0.3$–0.4, $M_1/M = 0.45$–0.55, and $M_1/M = 0.6$–0.7. The convention here is that M_1 denotes the mass of the fragment detected in PSAD1 at $\langle\theta\rangle = -55°$ and M_2 the mass of the fragment detected in PSAD2 at $\langle\theta\rangle = +55°$. M denotes the sum M_1+M_2.

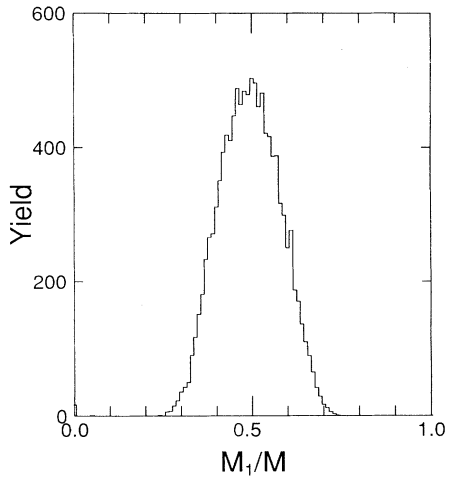

FIG. 1. Mass distribution for all triple f-f-α events. The mass M_1 of one of the fission fragments is presented as the fraction of the total mass of the composite system.

Figure 2 shows energy spectra of α particles measured at different angles in coincidence with fission fragments for the gate $M_1/M = 0.45$–0.55 corresponding to symmetric fission. The α-particle spectra were measured in the fission plane at azimuthal angles ranging (in 10° steps) from $\theta = 120°$ to 170° at one side of the beam and at $\theta = -160°$ and $-170°$ at the other side. For each spectrum the average value of the angle ψ_1 between the velocity vector of the fragment of the mass M_1 and the α particle (in the rest frame of the fissioning nucleus) is given in Fig. 2. The energy spectra are presented as the distributions of α-particle multiplicity per fission event and per unit solid angle, $d^2M/d\Omega\, dE$.

The solid curves shown in Fig. 2 represent results of calculations in which only prefission α emission [mechanism (i)] and the emission from separated, fully accelerated fragments [mechanism (iii)] were assumed. Contributions from these two mechanisms are shown by the dashed and dotted lines, respectively. It should be noted that the α particles from the fission fragments (dotted lines) have two clearly separated components associated with the in-flight emission from the two fragments moving in opposite directions.

The calculations of the α-particle evaporation from the composite system and from the fission fragments were done with the code CASCADE [13]. Only the prefission component turned out to be sufficiently sensitive for a determination of a best-fit value of the level-density parameter, $a = A/13$ MeV^{-1}. We have found, however, that the standard CASCADE calculation predicts the position of the maximum of the spectra at an energy that is systematically too high by about 2 MeV. The lowering of the effective Coulomb barrier for α particles evaporated from heavy composite systems was systematically ob-

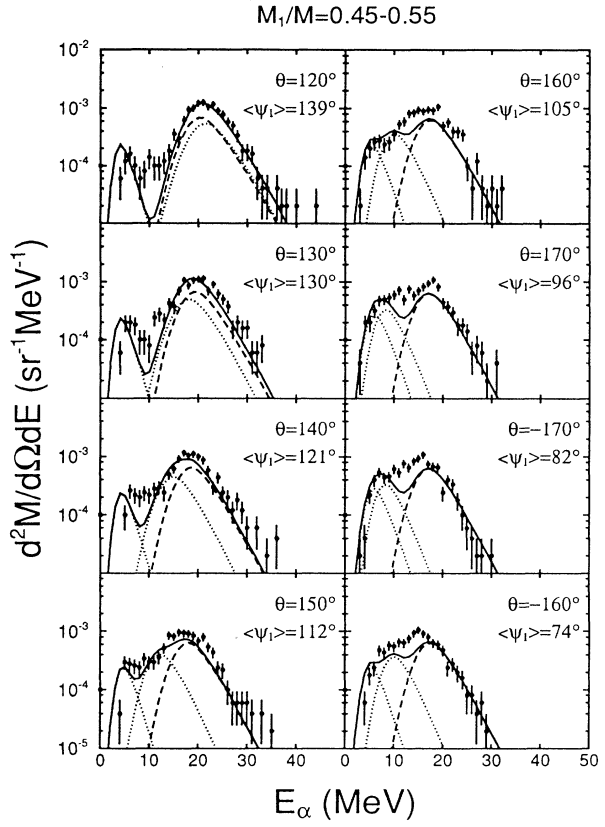

FIG. 2. Energy spectra of α particles measured at different angles, in coincidence with fission fragments, for symmetric fission ($M_1/M = 0.45$–0.55). ψ_1 denotes the angle between the velocity vector of the fragment of mass M_1 and the α particle (in the rest frame of the fissioning nucleus). The solid curves represent the combined effect of the prefission emission (dashed lines) and the emission from fully accelerated fragments (dotted lines).

served by Alexander, Guerreau, and Vaz [14] and also in the recent study by Ikezoe *et al.* [15]. In our statistical-model calculations, we artificially adjusted the position of the maximum of the calculated spectra by decreasing the effective Coulomb barrier by 1.8 MeV. The CASCADE calculations of the α-particle spectra from the fission fragments were done in a standard way as there is no indication so far for significant deviations from the statistical-model predictions for this medium-mass region of nuclei.

The calculated energy spectra were transformed to the laboratory reference frame as shown in Fig. 2. Isotropic angular distributions in the rest frame of the emitting nuclei were assumed for the α particles detected in the plane of the fission fragments. With this assumption the calculated spectra were normalized to the measured multiplicity distributions. As is seen from Fig. 2, the combined yield from the three assumed sources of α particles, shown by solid lines, reproduce quite consistently the observed distributions; however, in a limited angular range a considerable excess of the observed yields above the predictions is present. This excess is observed at energies of the α particles several MeV below the maximum of the component originating from the composite system prior to fission [mechanism (i)].

We emphasize that it is not possible to explain the observed excess of the α-particle yield within standard statistical-model calculations if the α-particle emission is allowed only from three clearly defined sources: the combined compound nucleus and both fission fragments. Our data show that there must be an additional source of α particles present that moves approximately with the velocity of the compound nucleus but that emits on average α particles of lower energies, preferentially in directions perpendicular to the fission axis. Such an additional source can be identified [8] with the emission of α particles at the near-scission stage from the neck region, a process known from neutron-induced and spontaneous fission of heavy nuclei. In the following analysis, we shall concentrate on the postulated mechanism of the near-scission emission of α particles, with the aim of providing convincing evidence of the presence of this mechanism.

Figure 3 shows the same data as presented in Fig. 2 in comparison with calculations in which the postulated α emission from the neck region [mechanism (ii)] is included in addition to the standard mechanisms (i) and (iii). We have parametrized the energy spectra of α particles originating from mechanism (ii) in such a way that they

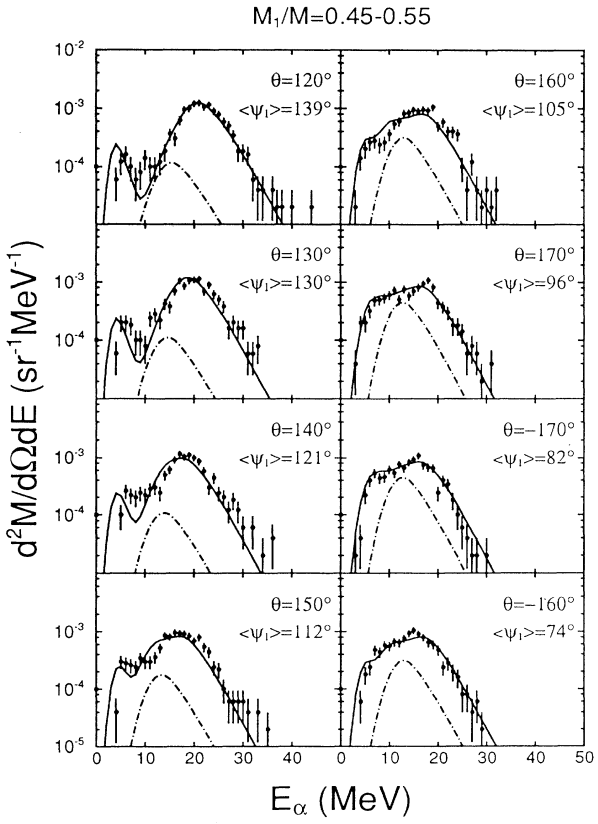

FIG. 3. Same as Fig. 2, except that the solid lines represent the combined effect of the prefission and postscission emissions (as shown in Fig. 2) plus the effect of the near-scission emission (dot-dashed lines).

have the same shape as for mechanism (i), i.e., the evaporation from the compound nucleus prior to fission, but the effective Coulomb barrier is arbitrarily shifted down by 5.5 MeV. [In the center-of-mass system, the maximum of the spectrum for mechanism (i) is at 25.2 MeV and for mechanism (ii) at 19.7 MeV.] The yield of the additional component was determined individually for each detection angle by requiring the best fit of the combined yield of the assumed mechanisms (i), (ii), and (iii) to the data. The contributions of mechanism (ii) are drawn in Fig. 3 by the dot-dashed lines, and the combined yield of all the components is shown by the solid lines.

Figure 4 shows the angular dependence of the component associated with mechanism (ii), i.e., the near-scission emission. We recall that ψ is the angle between the velocity vector of the α particle and the fission axis, measured in the rest frame of the fissioning nucleus. Figure 4 demonstrates that the α particles originating from mechanism (ii) are emitted preferentially in the direction perpendicular to the fission axis.

In Fig. 5 we show results of the measurements at a fixed angle $\theta=-170°$ ($\psi_1=82°$), i.e., close to the position of the maximum of the angular distribution in Fig. 4, but for different out-of-plane angles $\phi=0°$, 40°, and 60°. The meaning of the displayed curves is the same as for the results of the in-plane measurements displayed in Figs. 2 and 3. It is seen that the contribution of mechanism (ii), which is necessary to fit the total yields, practically does not change with the increasing angle ϕ. This indicates that the α particles originating from the neck region are emitted nearly isotropically in the plane perpendicular to the fission axis.

So far, we have concentrated on the analysis of the ternary fission events $f+f+\alpha$, characterized by the symmetric mass division $M_1/(M_1+M_2)=0.45-0.55$. Taking into account the necessity to provide decisively convincing evidence of the postulated near-scission α emission, it is essential to obtain information on the angular

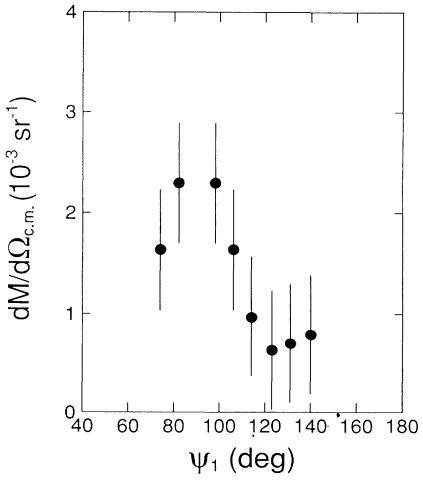

FIG. 4. In-plane angular distribution of the near-scission emission component for symmetric fission ($M_1/M=0.45-0.55$).

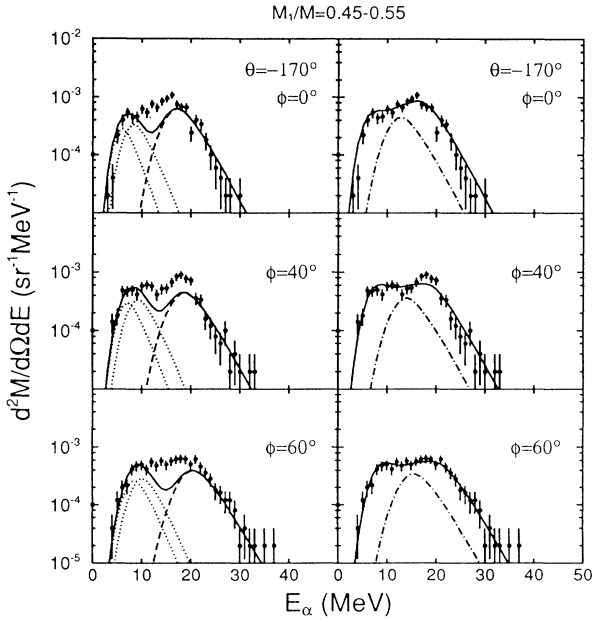

FIG. 5. Out-of-plane dependence of the energy spectra of α particles for symmetric fission ($M_1/M=0.45-0.55$). On the left-hand side, experimental spectra are compared with the combined effect (solid lines) of the prefission (dashed lines) and postscission emissions (dotted lines); on the right-hand side, the effect of the near-scission emission (dot-dashed lines) is added.

correlation between the α particles and fission fragments for asymmetric mass divisions of the fissioning nucleus. Such information is presented in Figs. 6 and 7.

Figure 6 shows the energy spectra of α particles measured in all the fission-plane detectors in coincidence with fission fragments within the gate $M_1/M=0.3-0.4$, characterizing strongly asymmetric fission events with the lighter fragment detected at $\psi_1=0°$ and the heavier one at $\psi_1=180°$. In Fig. 7 presented are the energy distributions taken for the inverse situation $M_1/M=0.6-0.7$, with the heavy fragment detected at $\psi_1=0°$ and the light one at $\psi_1=180°$. The same statistical decay calculations as for the symmetric-fission measurements have been performed. The contributions from the prescission and postscission emissions, as well as the combined yield, are drawn in Figs. 6 and 7 by using the same convention as in Fig. 2. One can clearly see that the yield additional to that originating from the pre- and postscission emissions is moved from the direction perpendicular to the scission axis ($\psi_1=90°$) toward the lighter fragment: For $M_1/M=0.6-0.7$ the additional yield is located above $\psi_1=90°$ (at $\psi_1=100°-115°$), and for $M_1/M=0.3-0.4$ it is moved below $\psi_1=90°$. This effect clearly indicates the emission of the α particles from the neck region. Because of the stronger Coulomb repulsion from the heavy fragment, the trajectories of the α particles deviate from $\psi_1=90°$ and are inclined toward the side of the light fragment.

The results of our analysis are summarized in Table I. Presented are angle-integrated α multiplicities for the

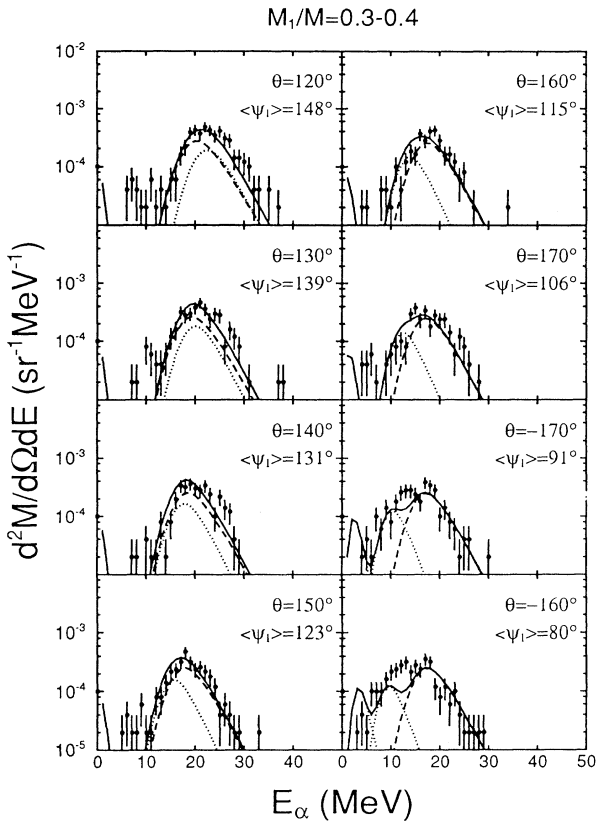

FIG. 6. Same as Fig. 2, except for asymmetric fission ($M_1/M=0.3$–0.4), i.e., with lighter fragments detected in detector 1.

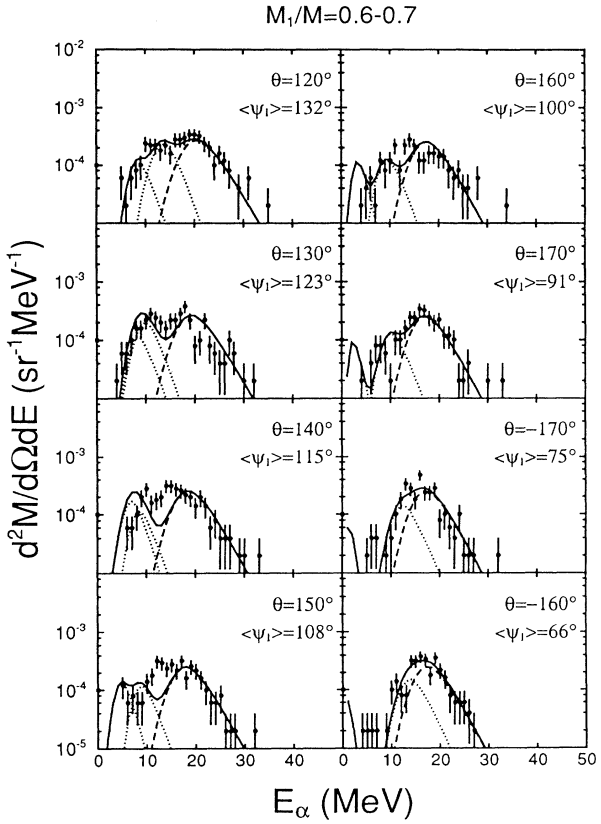

FIG. 7. Same as Fig. 2, except for asymmetric fission ($M_1/M=0.6$–0.7), i.e., with heavier fragments detected in detector 1.

prefission, postfission, and near-scission emissions for both symmetric and asymmetric fission. Extrapolations outside the fission plane were based on the out-of-plane measurements which showed a strong in-plane focusing for the prefission and postfission emissions and almost no dependence on the out-of-plane angle for the near-scission component.

Contrary to the differential distributions presented in Figs. 2–7, in which the α multiplicities have been calculated per one fission event indiscriminately of the mass ratio of the fission fragments (in order to illustrate relative yields of α particles), the angle-integrated multiplicities listed in Table I are related to the number of fission events within the actual gate imposed on the mass ratio.

IV. DISCUSSION AND CONCLUSIONS

The results presented in Table I should be compared with the existing fragmentary information on ternary fission induced by heavy ions. Sowinski *et al.* [5] presented a compilation of the existing results, showing a systematic trend of the increasing near-scission α multiplicity with the increasing excitation energy of the composite system in the range from about 0.002 for spontaneous fission and low-energy proton-induced fission ($E^*<50$ MeV) to about 0.01 for heavy-ion-induced fission at excitation energies $E^*\cong 200$ MeV. More recent results reported by Lindl *et al.* [6] also show the fast increase of the near-scission α multiplicity with the increasing excitation energy of the composite system (in the range between $E^*=100$ and 200 MeV). With the exception of a very small value of the near-scission α multiplicity at $E^*=100$ MeV ($M_\alpha=0.0007$), their results are consistent with the systematics [5].

The result of our measurement of the near-scission α multiplicity for the ^{40}Ar + ^{232}Th system ($E^*=183$ MeV), M_α (NSE)$\cong 0.035$, is well above some other data

TABLE I. Angle-integrated α-particle multiplicities for prefission, near-scission, and postfission emissions, M(pre), M(NSE), and M(post), respectively, given separately for symmetric and asymmetric fission. The errors in the multiplicities are due to uncertainties of the decomposition via the three-source calculation and the statistics.

	Symmetric fission	Asymmetric fission
M(pre)	0.17±0.03	0.22±0.05
M(NSE)	0.035±0.010	0.032±0.015
M(post)	0.09±0.02	0.06±0.03[a]
		0.10±0.03[b]

[a]Light fragment.
[b]Heavy fragment.

for the same range of excitation energies, generated however in much lighter composite systems [4,6]. It therefore seems that the formation of a highly charged composite system ($Z=108$) does increase the probability of the NSE mechanism. It should be noted here that a strong dependence of the α multiplicity on the fissility parameter Z^2/A is a well-known feature of ternary fission at low excitation energies [8].

As pointed out before, the possibility of measuring in the present experiment the emission of α particles as a function of the mass asymmetry of the fission fragments helped to unambiguously identify the near-scission emission mechanism. Moreover, the angle-integrated α-particle multiplicities for prefission, near-scission, and postfission emissions determined separately for symmetric and asymmetric fission (Table I) constrain reaction mechanisms. For instance, the values of the prefission α multiplicities seem to indicate, contrary to the suggestion in Ref. [3], that asymmetric fission is not faster than symmetric fission. The measured prefission α multiplicity for asymmetric fission (0.22 ± 0.05) is slightly larger than that for symmetric fission (0.17 ± 0.03), suggesting even a longer time of the asymmetric fission, although the difference is not significant due to large statistical errors.

The determination of the near-scission α multiplicities separately for symmetric and asymmetric fission (found to be about equal; see Table I), gives an additional independent argument in support of the conclusion that symmetric and asymmetric fission occur in approximately the same time. If asymmetric fission proceeded faster, the system would remain hotter in the near-scission configuration and one would expect more α particles emitted at that stage. In this argumentation we implicitly assume that the near-scission emission of α particles is evaporative in nature and thus depends on the available excitation energy, level density, etc., as in the standard statistical decay mechanism.

The concept of an evaporative nature of NSE has been put forward by Lindl *et al.* [6] on the basis of the observed scaling of the NSE multiplicities at different excitation energies with the prescission and postscission multiplicities. This concept invokes [6] a Coulomb-field-induced modulation of the evaporation barriers while the fragments are in close contact. Because of this effect, charged particles are evaporated preferentially in directions approximately perpendicular to the scission axis. The Coulomb focusing additionally enhances the effect of the sideward emission from the near-scission configurations.

Lindl *et al.* [6] pointed out that it is irrelevant, in a sense, whether to attribute the near-scission emission to the statistical emission from a strongly deformed composite system in its latest stage or from just separated fragments that are still in close proximity. However, as a matter of fact, the data on the near-scission emission carry very interesting information on the dynamics of fission. Consequently, the question of the origin and the emission time of the NSE particles can be attempted to be answered by carrying out time-dependent statistical-model calculations.

The time-dependent calculations have been done with a Monte Carlo statistical code SEQ [16]. The code has been modified in such a way that the mean lifetime corresponding to the total decay width, $\tau=\hbar/\Gamma_{\text{tot}}$, was calculated from the Weisskopf formula at each decay step. The decay time was then determined by sampling the corresponding distribution. In this way the time sequence along each Monte Carlo branch was obtained, and by averaging over all events the particle multiplicities as a function of time were determined.

Assuming the postscission scenario for the NSE α particles, one can relate the M(NSE) and M(post) multiplicities by

$$\tfrac{1}{2}M(\text{NSE})=M(\text{post})\int_0^{t_0}M_{ff}(t)dt\Big/\int_{t_0}^{\infty}M_{ff}(t)dt\ , \qquad (2)$$

where $M_{ff}(t)$ is the α-decay rate of a single fission fragment and t_0 is an effective time after which the fragments recede so far that the proximity effects influencing the near-scission emission vanish. (Here $t=0$ is taken to be the time of scission.) From a calculation with the code SEQ, we found that the time t_0 needed to explain the NSE component in terms of the postscission emission alone is about 1.8×10^{-21} s. (According to the systematics of Hinde *et al.* [17], the initial excitation energy of the fission fragments was assumed to be 70 MeV per fragment.) It is easy to check that during the time $t_0=1.8\times10^{-21}$ s the fragments will move from scission ($r\cong19$ fm) to a relative distance $r=41$ fm. However, the proximity effects must practically vanish already at smaller distances. Therefore we cannot attribute the NSE effect entirely to the postscission emission from separated fragments. It is reasonable to assume that the Coulomb-field-induced modulation of the evaporation barriers [6] and Coulomb focusing of α-particle trajectories give a visible effect while the fragments move from scission not further than for about 10 fm, i.e., up to a relative distance $r\cong29$ fm. This takes a time $t_0=1.1\times10^{-21}$ s. From Eq. (2) we find then that the postscission emission may account for about 65% of the observed magnitude of M(NSE).

We also checked to what extent the alternative process, i.e., the prescission emission, may contribute to the NSE α-particle multiplicity. In this scenario the relative magnitudes M(NSE) and M(pre) sensitively depend on the dynamics of fission, specifically on the total fission time τ_f (from the formation of the composite system to scission) and the time τ_{NSE} during which the system passes via strongly elongated shapes just before scission. The relation between the M(NSE) and M(pre) multiplicities can be written as

$$M(\text{NSE})=M(\text{pre})\int_{\tau_f-\tau_{\text{NSE}}}^{\tau_f}M_{\text{CS}}(t)dt\Big/\int_0^{\tau_f-\tau_{\text{NSE}}}M_{\text{CS}}(t)dt\ , \qquad (3)$$

where $M_{\text{CS}}(t)$ is the α-decay rate of the composite system that can be calculated with the program SEQ [16]. It is now well established that fission as a collective decay mode is rather slow (see, e.g., Refs. [18,17]), and therefore

at high excitation energies it cannot compete with fast statistical emission of neutrons and light charged particles. Therefore calculations of $M_{CS}(t)$ were done with complete suppression of fission. The systematics of the prescission neutron multiplicities ν_{pre} of Hinde *et al.* [19] were used as a "calibration clock" in the calculation. For $\nu_{pre}=9$ our calculation with the program SEQ gave the fission time $\tau_f \cong 6.8\times10^{-20}$ s assuming an initial excitation energy of the composite system $E^*=E_{c.m.}+Q(\text{fusion})\simeq 183$ MeV, increases gradually at the final stage preceding scission by an amount of energy E_{diss} that is dissipated on the descent from saddle to scission. The value of E_{diss} was estimated from the one-body dissipation model of Blocki *et al.* [20]. Depending on the angular momentum, E_{diss} predicted by the model [20] varies from 30 to 60 MeV for typical fusion trajectories leading to symmetric fission. An average value $E_{diss}=40$ MeV was used in the calculation. The time dependence of the E_{diss} generation, predicted by the dynamical model [20], was implemented into the program SEQ in such a way that the time of scission predicted by the model [20] was matched with the statistical decay time in SEQ corresponding to our calibration mark $\nu_{pre}=9$.

It should be noted here that the statistical model calculations are very sensitive to the timing of the "injection" of the additional energy E_{diss}. For example, if E_{diss} is assumed to be available already at the start of the calculation (as it was assumed in similar statistical-model calculations with the code JULIAN reported by Hinde *et al.* [17]), the multiplicity $\nu_{pre}=9$ is reached much faster, and so the fission time deduced in such a way is shorter, $\tau_f=3.0\times10^{-20}$ s. Our result with the generation of E_{diss} in the latest stage of fission ($\tau_f=6.8\times10^{-20}$ s for $\nu_{pre}=9$) only slightly differs from the calculation without inclusion of E_{diss} at all, $\tau_f=7.2\times10^{-20}$ s for $\nu_{pre}=9$. Therefore we conclude that the fission times deduced from the calculations with the code JULIAN [17] (in which E_{diss} is available from the very beginning) may be underestimated.

For the value of $\tau_f=6.8\times10^{-20}$ s (deduced from the calculation with the program SEQ), Eq. (3) gives an effective time of the near-scission emission $\tau_{NSE}=4.3\times10^{-20}$ s, provided that M(NSE) is entirely attributed to the emission prior to scission. In order to judge the meaning of the deduced time scales, we performed dynamical calculations with the one-body dissipation model of Blocki *et al.* [20] and extracted information on the predicted evolution of shapes as a function of time.

In the model [20] a colliding system is considered in a configuration space described by three parameters: a relative distance parameter $\rho=r/(R_1+R_2)$, a dimensionless parameter λ, being a measure of the degree of opening of the neck through which the fragments communicate, and a parameter $\Delta=(R_1-R_2)/(R_1+R_2)$, accounting for the asymmetry of the system. From the calculations we inferred that the time $\tau_{NSE}=4.3\times10^{-20}$ s [determined by assuming that M(NSE) is entirely due to the prescission emission] is definitely too long. For symmetric divisions ($\Delta=0$), it spans from a position in the configuration space $\rho=0.32$ and $\lambda=1.65$ to scission ($\rho=2.14$, $\lambda=0.53$). It is easy to check that in the starting point of this time interval the composite system still remains in the mononuclear regime. Following definitions of Blocki and Swiatecki [21], one can take as a limit of mononuclear shapes a "capped cylinder" or, for asymmetric divisions, a "capped cone" shape characterized by a 100% opening of the neck, $\alpha=[1-\rho(1-\lambda)]/(1-\Delta^2)$. In the deduced starting configuration ($\rho=0.32$, $\lambda=1.65$, $\Delta=0$), the opening is very large, $\alpha=121\%$, the neck region still remains convex, and consequently the α particles emitted at that stage cannot show features of NSE.

Similarly as in the case of the postscission interpretation of the NSE effect, we estimate a probable contribution of the prescission emission to the observed value of M(NSE). We assume that the NSE effect can be clearly seen only for elongated dinuclear shapes with a well-developed concave neck between the fragments, say, for shapes with an opening $\alpha\leq 75\%$. For this criterion the dynamics calculation [20] gives $\tau_{NSE}=0.6\times10^{-20}$ s. By using then the code SEQ, we find from Eq. (3) that about 40% of the observed NSE effect can be attributed to the prescission emission. It should be emphasized that also this result sensitively depends on the timing of E_{diss}. Because of the generation of E_{diss} at the last stage of fission, the calculation predicts a significant increase of the α emission at that stage. This indicates that the magnitude of E_{diss} is one of the key factors determining the NSE effect.

Summarizing the discussion on the time scale and sequence of events in the near-scission emission, we conclude that the measured intensities of the near-scission as well as pre- and postscission emissions of α particles are consistent with the interpretation of the NSE component in terms of standard statistical evaporation. The time-dependent statistical-model calculations show that the magnitude of the near-scission multiplicity M(NSE) is well explained as a combined effect of the evaporation during the descent of the composite system to scission and the evaporation from separated fragments immediately after scission. The calculations suggest that contributions of the two processes have comparable magnitudes. Since the predicted rates of the evaporation processes practically exhaust the whole NSE effect, there is no necessity to postulate the existence of an additional nonevaporative mechanism acting during scission, e.g., a snapping of the neck shortly after scission proposed by Halpern [22], as an explanation of ternary fission at low excitation energies.

As pointed out by Lindl *et al.* [6], staying on the grounds of the evaporative mechanism, the strong concentration of NSE in directions perpendicular to the scission axis cannot be explained entirely in terms of three-body Coulomb trajectory calculations with an assumed isotropic emission of α particles from the fragments. It is necessary to assume [6] a Coulomb-field-induced modulation of the evaporation barriers when the fragments are in close proximity. Our analysis, confirming the evaporative nature of the NSE, indirectly supports the concept of the barrier modulation.

Finally, it should be emphasized that the measured prescission evaporation multiplicities combined with

time-dependent statistical-model calculations give a time scale of the fusion-fission process that is consistent with predictions of classical dynamical calculations based on the one-body dissipation model [20]. In both approaches fission of the hot composite systems turns out to be rather slow: It lasts about 5–7 units of 10^{-20} s and therefore during that time cannot compete with evaporation of light particles. Measurements of the near-scission emission allow us, additionally, to deduce information on the time scale of fission in its final stage, starting from a moment when a dinuclear system (with a concave neck) is formed. Our results indicate that this time scale is in the range from 5×10^{-21} to 8×10^{-21} s, which is consistent with predictions of the one-body dissipation model [20], and show that the kinetic energy generated during the descent to scission is damped almost completely.

ACKNOWLEDGMENTS

The authors would like to thank Jan Blocki for providing us with his model predictions. This work was performed as a part of the research program of the Stichting voor Fundamenteel Onderzoek der Materie (FOM) with financial support of the Netherlandse Organisatie voor Wetenschappelijk Onderzoek (NWO). Financial support of the Committee of Scientific Research of Poland (KBN Grant No. 2-00899101 and funds Nos. 621/E91/92 and BST 411/92) is also acknowledged.

[1] M. Gonin, L. Cooke, K. Hagel, Y. Lou, J. B. Natowitz, R. P. Schmitt, S. Shlomo, B. Srivastava, W. Turmel, H. Utsunomiya, R. Wada, G. Nardelli, G. Nebbia, G. Viesti, R. Zanon, B. Fornal, G. Prete, K. Niita, S. Hannuschke, P. Gonthier, and B. Wilkins, Phys. Rev. C **42**, 2125 (1990).

[2] J. P. Lestone, J. R. Leigh, J. O. Newton, D. J. Hinde, J. X. Wei, J. X. Chen, S. Elfstrom, and D. G. Popescu, Phys. Rev. Lett. **67**, 1078 (1991).

[3] E. Duek, N. N. Ajitanand, J. M. Alexander, D. Logan, M. Kildir, L. Kowalski, L. C. Vaz, D. Guerreau, M. S. Zisman, M. Kaplan, and D. J. Moses, Z. Phys. A **317**, 83 (1984).

[4] L. Schad, H. Ho, G. Y. Fan, B. Lindl, A. Pfoh, R. Wolski, and J. P. Wurm, Z. Phys. A **318**, 179 (1984).

[5] M. Sowinski, M. Lewitowicz, R. Kupczak, A. Jankowski, N. K. Skobelev, and S. Chojnacki, Z. Phys. A **324**, 87 (1986).

[6] B. Lindl, A. Brucker, M. Bantel, H. Ho, R. Muffler, L. Schad, M. G. Trauth, and J. P. Wurm, Z. Phys. A **328**, 85 (1987).

[7] H. Ikezoe, N. Shikazono, Y. Nagame, T. Ohtsuki, Y. Sugiyama, Y. Tomita, K. Ideno, I. Kanno, H. J. Kim, B. J. Qi, and A. Iwamoto, in *Proceedings of the Fourth International Conference on Nucleus-Nucleus Collisions,* Kanazawa, Japan, 1991, edited by H. Toki, I. Tanihata, and H. Kamitsubo, [Nucl. Phys. **A538**, 299c (1992)].

[8] R. Vandenbosch and J. R. Huizenga, *Nuclear Fission* (Academic, New York, 1973).

[9] J. P. Theobald, P. Heeg, and M. Mutterer, in *Proceedings of the International Conference on Fifty Years Research in Nuclear Fission,* Berlin, Germany, 1989, edited by D. Hilscher, H. J. Krappe, and W. von Oertzen, [Nucl. Phys. **A502**, 343c (1989)].

[10] P. C. N. Crouzen, Ph.D. thesis, University of Groningen, 1988.

[11] V. E. Viola, K. Kwiatkowski, and M. Walker, Phys. Rev. C **31**, 1550 (1985).

[12] J. Lukasik, S. Micek, Z. Sosin, A. Wieloch, and K. Grotowski, Nucl. Instrum. Methods A **274**, 265 (1989).

[13] F. Pühlhofer, Nucl. Phys. **A280**, 267 (1977).

[14] J. M. Alexander, D. Guerreau, and L. C. Vaz, Z. Phys. A **305**, 313 (1982).

[15] H. Ikezoe, N. Shikazono, Y. Nagame, Y. Sugiyama, Y. Tomita, K. Ideno, A. Iwamoto, and T. Ohtsuki, Phys. Rev. C **42**, 342 (1990).

[16] H. W. Wilschut (unpublished).

[17] D. J. Hinde, D. Hilscher, H. Rossner, B. Gebauer, M. Lehmann, and M. Wilpert, Phys. Rev. C **45**, 1229 (1992).

[18] J. B. Natowitz, M. Gonin, M. Gui, K. Hagel, Y. Lou, D. Utley, and R. Wada, Phys. Lett. B **247**, 242 (1990).

[19] D. J. Hinde, H. Ogata, M. Tanaka, T. Shimoda, N. Takahashi, A. Shinohara, S. Wakamatsu, K. Katori, and H. Okamura, Phys. Rev. C **39**, 2268 (1989).

[20] J. Blocki, R. Planeta, J. Brzychczyk, and K. Grotowski, Z. Phys. A **341**, 307 (1992).

[21] J. Blocki and W. J. Swiatecki, Lawrence Berkeley Laboratory Report No. LBL-12811, Berkeley, 1982.

[22] I. Halpern, Annu. Rev. Nucl. Sci. **21**, 245 (1971).